PATTERNS OF GLAUCOMATOUS VISUAL FIELD LOSS IN SITA FIELDS AUTOMATICALLY IDENTIFIED USING INDEPENDENT COMPONENT ANALYSIS

BY **Michael H. Goldbaum MD**,* Gil-Jin Jang PhD, Chris Bowd PhD, Jiucang Hao PhD, Linda M. Zangwill PhD, Jeffrey Liebmann MD, Christopher Girkin MD, Tzyy-Ping Jung PhD, **Robert N. Weinreb MD,** AND Pamela A. Sample PhD

ABSTRACT

Purpose: To determine if the patterns uncovered with variational Bayesian–independent component analysis–mixture model (VIM) applied to a large set of normal and glaucomatous fields obtained with the Swedish Interactive Thresholding Algorithm (SITA) are distinct, recognizable, and useful for modeling the severity of the field loss.

Methods: SITA fields were obtained with the Humphrey Visual Field Analyzer (Carl Zeiss Meditec, Inc, Dublin, California) on 1,146 normal eyes and 939 glaucoma eyes from subjects followed by the Diagnostic Innovations in Glaucoma Study and the African Descent and Glaucoma Evaluation Study. VIM modifies independent component analysis (ICA) to develop separate sets of ICA axes in the cluster of normal fields and the 2 clusters of abnormal fields. Of 360 models, the model with the best separation of normal and glaucomatous fields was chosen for creating the maximally independent axes. Grayscale displays of fields generated by VIM on each axis were compared. SITA fields most closely associated with each axis and displayed in grayscale were evaluated for consistency of pattern at all severities.

Results: The best VIM model had 3 clusters. Cluster 1 (1,193) was mostly normal (1,089, 95% specificity) and had 2 axes. Cluster 2 (596) contained mildly abnormal fields (513) and 2 axes; cluster 3 (323) held mostly moderately to severely abnormal fields (322) and 5 axes. Sensitivity for clusters 2 and 3 combined was 88.9%. The VIM-generated field patterns differed from each other and resembled glaucomatous defects (eg, nasal step, arcuate, temporal wedge). SITA fields assigned to an axis resembled each other and the VIM-generated patterns for that axis. Pattern severity increased in the positive direction of each axis by expansion or deepening of the axis pattern.

Conclusions: VIM worked well on SITA fields, separating them into distinctly different yet recognizable patterns of glaucomatous field defects. The axis and pattern properties make VIM a good candidate as a preliminary process for detecting progression.

Trans Am Ophthalmol Soc 2009;107:136-145

INTRODUCTION

Knowing whether an eye with glaucoma is stable or progressing is perhaps the most important information for the clinician who is managing a patient with glaucoma. We previously applied a modified form of independent component analysis (ICA) to visual field results obtained with standard automated perimetry (SAP) full threshold from 345 normal and glaucomatous eyes to discern patterns of visual field loss in glaucoma.[1,2] That method was then used to detect progression in sequential full-threshold perimetry.[3] We now apply the same method to eyes tested with the Swedish Interactive Thresholding Algorithm (SITA).

Discovering the structure in a set of data can provide instructive information about the data (data mining). Segmenting the structure of the data can also serve as a preparatory step for a specific task, for example, detecting change. The components of the data can be decomposed by different types of unsupervised learning into various structures; clusters and axes are two examples of ways to represent the data organization. We reported that representing visual field patterns solely as clusters by the process of mixture of factor analysis could uncover different patterns of visual field loss, but such grouping was limited in that early losses were placed in several clusters while more advanced patterns were put in a different cluster.[4] We discovered that representing visual fields using a modification of ICA was a particularly good way to separate cross-sectional field results. ICA not only separated the fields by pattern of loss, but also organized fields from mild to advanced versions of the same pattern along an axis representing that particular pattern.[1-3] That property then enabled us to look for progression of glaucomatous field loss by focusing on the pattern that was most significant for a given patient.[3]

Recently, the new, faster SITA has become the standard for the perimetric assessment of standard visual fields for glaucoma.[5] In this study, we report the separation of visual field patterns by a modified ICA for 2,085 normal and glaucoma eyes tested with SITA; this represents a set 6 times larger than the previous set. Our adaptation of ICA is the *v*ariational Bayesian–*i*ndependent component analysis–*m*ixture model (now named VIM).[6,7] We report the application of VIM to the larger database of SITA fields to find maximally independent glaucomatous patterns in which we can identify levels of severity as preparation for detecting glaucomatous field progression by the progression of patterns (POP) process.[8] POP is currently under investigation as a separate project.

METHODS

PARTICIPANT SELECTION AND TESTING

Participants

This study employed the SITA visual field set collected for 6 years from two longitudinal studies sponsored by the National Eye

*Presenter.

Bold type indicates AOS member.

From the Department of Ophthalmology (Dr Goldbaum, Dr Bowd, Dr Zangwill, Dr Weinreb, Dr Sample) and Institute for Neural Computation (Dr Jang, Dr Hao, Dr Jung), University of California San Diego; the New York Eye and Ear Infirmary, New York, New York (Dr Liebmann); and the University of Alabama at Birmingham (Dr Girkin).

Institute—the Diagnostic Innovations in Glaucoma Study (DIGS) at the University of California, San Diego (UCSD), and the multicenter African Descent and Glaucoma Evaluation Study (ADAGES) acquired at UCSD, the New York Eye and Ear Infirmary, and the University of Alabama at Birmingham. Normal participants for this study were recruited from the community, staff, and spouses or friends of patients. Informed consent was obtained from all participants. The study followed the tenets of the Declaration of Helsinki and was approved by the Institutional Review Boards of the 3 universities.

Exclusion criteria for both groups included unreliable visual fields (defined as >33% for either fixation loss, false-negative errors, or false-positive errors), angle abnormalities on gonioscopy, diseases other than glaucoma that could affect the visual fields, medications known to influence visual field sensitivity, and poor-quality stereoscopic photographs of the optic disc. Eyes with a best-corrected visual acuity worse than 20/40, spherical equivalent outside of ±5.0 diopters, and cylinder correction greater than 3.0 diopters were excluded. A family history of glaucoma was not an exclusion criterion.

Normal visual fields were obtained from subjects who were recruited or referred as normal. Inclusion criteria for the "normal" category required that subjects have intraocular pressures of less than 22 mm Hg, no history of elevated intraocular pressure or use of pressure-lowering medication, normal SITA fields (see glaucomatous field criteria below), and no evidence of glaucomatous optic neuropathy on simultaneous stereoscopic photographs. Normal optic discs had a cup-disc ratio asymmetry of 0.2 or less, intact rims without hemorrhages or evidence of notching or excavations, and the absence of visible nerve fiber layer defects in the adjacent retina or evidence of any other pathology. Inclusion criteria for the glaucoma field category required a glaucoma hemifield test (GHT) "outside normal limits" or pattern standard deviation (PSD) at 5% or worse on 2 consecutive visual field tests.

The Indicator of Glaucoma for Posthoc Analysis

In the first application of VIM on SAP full threshold, glaucomatous optic neuropathy alone was used as an indicator of glaucoma.[1,2] Some eyes with glaucomatous visual fields have normal discs and some eyes with glaucomatous optic neuropathy have normal fields, resulting in built-in false-positive and false-negative rates that increase the difficulty of validating unsupervised learning. The goal of this project is not to diagnose glaucoma but to separate glaucomatous SITA fields into maximally different patterns and to establish a method of data representation that allows for the detection of progression. The designation of an eye by GHT and PSD as glaucomatous or normal was used in post hoc validations to select the VIM model that best separated normal and glaucomatous visual fields.

REPRESENTATION OF THE DATA BY VIM

Input for the Classifier

All subjects were measured with SAP with the Humphrey Visual Field Analyzer (HFA; Carl Zeiss Meditec, Inc, Dublin, California) using the 24-2 program and the SITA.[5] The values extracted from the 52 perimetric locations (2 blind spot locations not included) were the absolute sensitivity, the total deviation, and the pattern deviation. Comparison of machine learning classifiers trained with these 3 types of input found no significant difference in classifier performance; hence, absolute sensitivities (52 input nodes) plus age (one input node) were the sole input to VIM. Age was included because both normal and glaucomatous SITA fields expressed as absolute sensitivity are affected by age, and age was used successfully in the previous studies of classifiers with supervised and unsupervised learning.[1,3,9-11] The absolute sensitivity (in decibels) of the 52 visual field locations plus age (years) formed a vector in 53-dimensional input space for each of the 2,085 SITA fields.

Partitioning Data Into Clusters and Adjusting Axes Within the Clusters

The unsupervised learning was performed with the VIM.[1,2] This method forms the basis for our technique for improving the detection of glaucomatous visual field deterioration. A detailed, mathematically rigorous description of VIM is available in the "Appendix" section of the AOS thesis by Goldbaum[1] or in studies detailing its use with full-threshold SAP fields.[2,6] A summary description follows.

Independent component analysis alone seeks one set of axes; ICA applied to a set of normal and abnormal fields would create one set of axes for the entire data set. We previously determined that better segmentation of the glaucomatous field patterns is achieved by separating the axes for abnormal eyes from the axes for normal eyes.[1,2] The mixture model of ICA creates clusters and simultaneously seeks an optimal set of axes representing maximally independent patterns within each cluster. Bayesian learning is applied to overcome overfitting by maximum likelihood estimation. The cluster assignments and axis adjustments are iterated until no further change occurs in the cluster assignment.[6,7] VIM combines ICA, the mixture model, and Bayesian learning. The output is clusters and the axes generated and oriented within each cluster. It is the properties of the fields associated with the axes that define the patterns we are seeking.

Starting with the 2,085 subjects evenly distributed in c clusters and with random initialization of the axes, VIM learned the orientation of the axes and the probability distribution of each cluster. The initiating variables for the learning process were the number of clusters, c, and, within each cluster, the number of axes and number of Gaussian surfaces (to model the distribution of the data for the mixture model). From c = 2-5, we found c = 2 or 3 gave better separation of normal and glaucoma fields. At the beginning of learning, the number of clusters was therefore set at c = 2 or 3, the number of axes in each cluster was 10, 20, or 30, and the number of Gaussians in each cluster was 3 or 8. This yielded 12 starting combinations. Thirty random initializations were tried for each starting combination, giving a total of 360 models tried.

The goal was to reduce the error in structure representation (global minimum or a minimum close to the global minimum of the error surface). The possibility of ending up in a high local minimum was diminished by identifying the model with the best separation of normal and abnormal fields from the 360 different models. The process was designed to be automatic, with minimal human

intervention. For each of the 360 models, 500 iterative adaptation steps were carried out. For each SITA field, its cluster assignment during convergence was then recomputed according to its likelihood value given by VIM. The clusters split and merged during convergence; the number of axes and Gaussians did not change. Fields belonging to the same cluster defined the mean and axes for that cluster.

After convergence, sensitivity [proportion of abnormal fields in cluster(s) that were mostly abnormal] and specificity [proportion of normal fields in cluster(s) that were mainly normal] were used post hoc to choose the 5 best models, and the convergence of evidence value was used to select the top model from those 5. At this stage, the top model had 3 clusters, 10 axes per cluster, and 3 Gaussians per cluster.

Of the 10 axes per cluster, poorly contributing axes were pruned. The axes in each cluster were sorted by the magnitude of their contribution and graphed by axis contribution vs number of axes to determine the number of axes beyond which little further gain in contribution would be obtained (at the knee in Figure 1). Axes beyond the knee were removed. The model then relearned the clusters and axis orientations with only the contributing number of axes in each cluster.

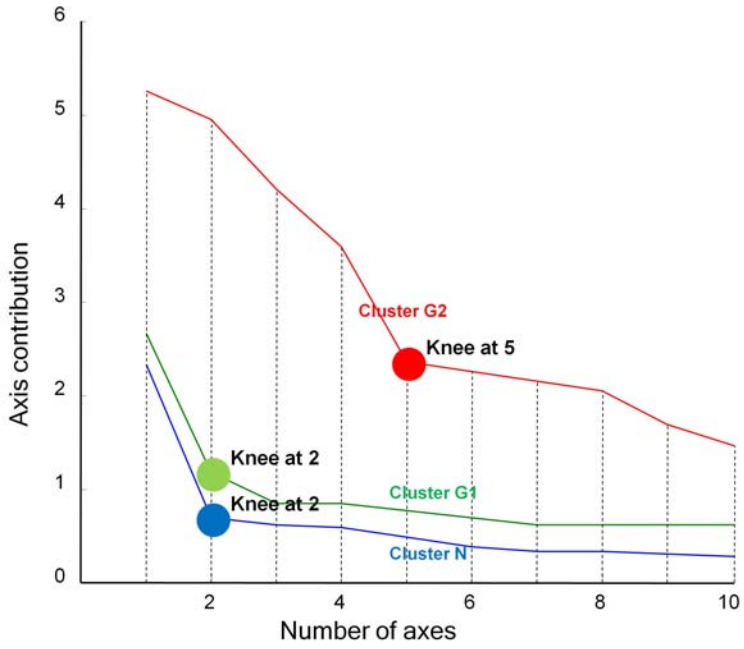

FIGURE 1

Plot of axis contribution to VIM vs number of axes. Axes beyond knee were removed, leaving 2 axes each for clusters 1 and 2 and 5 axes for cluster 3. VIM was re-initialized, constrained to the reduced number of axes.

POST HOC ANALYSIS

Validation of Structure

VIM does not know the class identity of the fields at the time it creates the clusters and orients the axes. Validation is done after learning the clusters and axes (post hoc) by observing how well the classifier outcome conforms to expectations. The process is validated by observing whether the structure obtained by VIM is appropriate for the data. Because the data contain normal and abnormal visual fields, we first evaluate the clusters for their proportion of each. The second validation comes from the evaluation of axes created and oriented by VIM within each cluster and from the examination of the fields associated with each axis.

The distribution of normal and abnormal fields in each cluster is used to select the best VIM model. The expectation is that the model that best separates the normal and glaucoma fields with the fewest false-negatives and false-positives is the best model for creating axes. The axes created within each cluster by the best model are then examined for patterns consistent with glaucoma, for the distribution of severity along an axis, and for the distinctiveness of the patterns in different axes.

Evaluating the Axes

Representing the visual field patterns as axes through each cluster mean organizes the field loss patterns from mild to severe.[1-3] Visual field experts typically rely on the total deviation (TD) or pattern deviation (PD) plots supplied by the HFA Statpac analysis (Carl Zeiss Meditec, Inc, Dublin, California), which takes into account the deviation from age-matched healthy eyes (TD) and additionally the effect on the fields of global factors such as cataract (PD). The numerical plots were displayed as TD-like plots at –2, 0 (cluster mean), and +2 SD along each of the axes. The numerical TD-like plots were converted into grayscale representations that allowed the patterns associated with each axis to be visualized. The maximum TD depression of the VIM-generated plots was –21. The –7 to –21 values

were displayed as equal steps of gray, with −7 the lightest and −21 as black. The TD-like plots and grayscale displays for the VIM-generated fields on each axis were examined independently by 2 experts (P.A.S., M.H.G.) for distinctiveness of the axes and for resemblance of the VIM-generated patterns to patterns normally associated with glaucoma.

Associating SITA Fields With an Axis

Each individual eye, located in 53-dimensional input space by the 52 visual field locations and age, is projected on each of the ICA axes. The size of the projection on each axis is measured in units of standard deviation. The SITA visual fields within each cluster are segmented into groups by assigning each field to the one axis on which the projection of the field yields the maximum value in standard deviations. The fields associated with an axis are sorted by their projection on the axis from the most minus to the most plus and displayed for examination. Displaying the SITA fields from most minus to most plus organizes them from earliest field defects to most advanced field defects.[1-3]

The maximum TD depression of all 2,085 SITA fields was −31 dB. The −7 to −31 values in the grayscale are displayed in equal steps of gray, with −7 the lightest and −31 as black. The SITA fields were noted for their resemblance to the generated fields on the axis, to the other SITA fields associated to the same axis, and to consistency in increasing severity as the fields were located further in the positive direction along the axis.

RESULTS

CLUSTERS CREATED BY VIM

Of the 360 models of VIM, the chosen model contained 3 clusters. Figure 2 shows a two-dimensional demonstration of clusters 1, 2, and 3 collapsed from the 53 dimensions in input space. The 3 clusters overlap, and each cluster has an ellipsoidal distribution. Cluster 1 was made up of mostly normal eyes (1,089 of 1,183). The average mean defect (MD) was −0.54 ± 1.32 SD. The fields in cluster 2 were minimally abnormal. The average MD was −2.16 ± 1.58. The fields in cluster 3 were relatively more severely abnormal. The average MD was −8.4 ± 6.42.

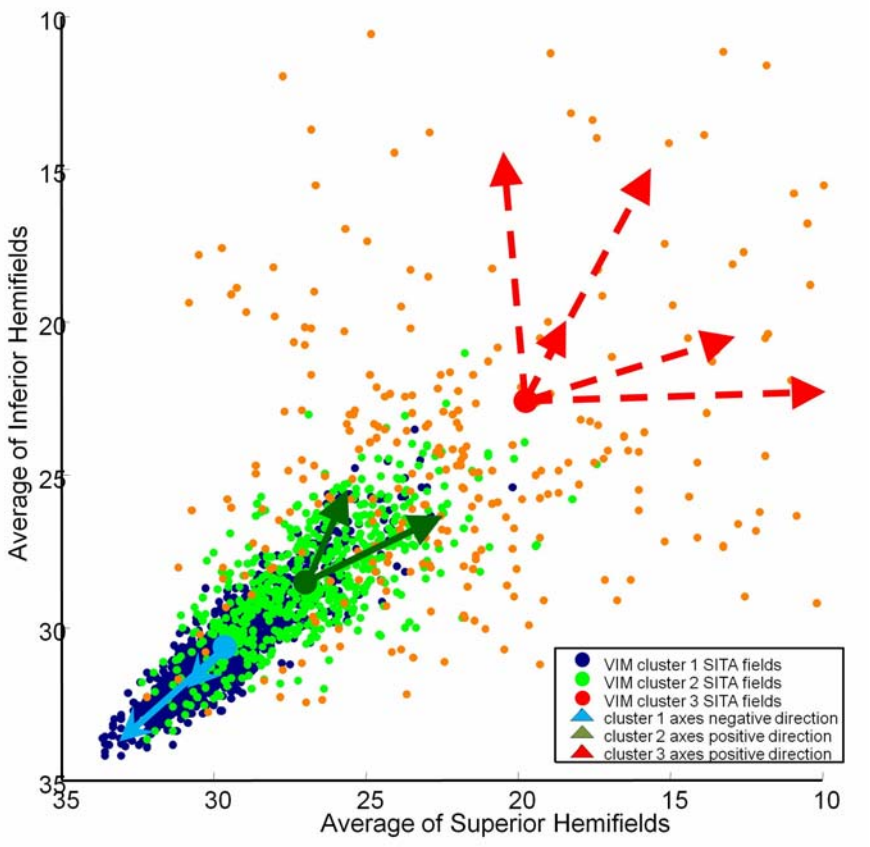

FIGURE 2

Two-dimensional view of original 53-dimensional input space created by using the average absolute sensitivity of the superior field locations vs the average absolute sensitivity of the inferior field locations plus age. Centroids (cluster means) and the distribution of SITA fields are displayed for clusters 1 (blue), 2 (green), and 3 (red). Axes go through centroid in each cluster. Positive direction for each axis is away from the cluster 1 centroid; negative is generally opposite. To prevent overlap, display shows negative side of axes for cluster 1 and positive side of axes for clusters 2 and 3. Units on each axis are in standard deviations (not displayed).

The distribution of normal and abnormal fields is presented in Table 1. Cluster 1 contained 1,193 fields (1,089 normal and 104 abnormal fields), cluster 2 contained 569 fields (56 normal and 513 abnormal), and cluster 3 contained 323 fields (1 normal and 322 abnormal). Post hoc combination of clusters 2 and 3 yielded a sensitivity of 88.9% for placing abnormal fields in cluster 2 or cluster 3 and a specificity of 95.0% for placing normal fields in cluster 1. Of the 2 clusters containing mostly abnormal fields (clusters 2 and 3), cluster 2 had 63.8% of the eyes and cluster 3 had 36.2%.

TABLE 1. DISTRIBUTION OF SITA FIELDS

FIELD RESULTS	CLUSTER 1	CLUSTER 2	CLUSTER 3	ALL CLUSTERS
Normal	1089	56 (FP)	1 (FP)	1146
Abnormal	104 (FN)	513	322	939
Total	1193 (57.2% of 2085)	569 (27.3% of 2085)	323 (15.5% of 2085)	2085
	Specificity 95.0%	Sensitivity 88.9%		

FN, false-negative; FP, false-positive; SITA, Swedish Interactive Thresholding Algorithm.

AXES CEATED BY VIM

All the information in the SITA field data set was represented by 9 maximally independent axes. Separating the patterns on positive and negative sides of the cluster mean yielded 18 patterns. Cluster 1 and cluster 2 each contained 2 axes, and cluster 3 had 5 axes (Figure 1). Most of the normal fields were represented by 2 axes in cluster 1, and most of the glaucomatous fields were expressed by 7 axes in clusters 2 and 3; this gave rise to 14 patterns in the abnormal fields. In Figure 2, the VIM-derived axes are superimposed on the clusters, showing the axes in each cluster passing through the cluster mean.

Analysis of Generated Patterns Along Axes

The numerical plots associated with each visual field generated by VIM at particular points on each axis in the VIM multidimensional space are equivalent to absolute sensitivity plots. These plots are converted to simulate numerical TD plots by subtracting the VIM-generated absolute sensitivity plot of the mean of cluster 1, the cluster holding nearly all of the normal eyes, from the VIM-generated absolute sensitivity plot at particular points on each axis. Another way of considering the simulated total deviation plot is as a 53-dimensional vector originating at the centroid of cluster 1 and ending at the specified point on a given axis.[1,2]

Cluster 1 contained 95% of the normal eyes and 11.1 % of the glaucomatous eyes. The generated pattern at the centroid of cluster 1 could be considered the mean normal visual field. Since this pattern was the one used for transforming absolute sensitivity plots to TD-like plots, transforming itself to resemble a total deviation plot by definition resulted in 0 dB in all locations, and its grayscale showed white at all locations (Figure 3). The generated fields at –2 and +2 SD on axis 1 were uniformly mildly depressed (–3 dB) or above normal (+3 dB), respectively. The generated fields at –2 and +2 SD on axis 2 were almost the same (within ±1 dB) as the VIM-generated normal mean.

The generated mean glaucoma field in cluster 2 had a MD of –2.44 dB (compared to –2.16 average MD for all the SITA fields in cluster 2), with a superior to inferior ratio of 1.23. The grayscale of the mean of cluster 2 had mild generalized depression with a slightly deeper superior arcuate defect. The pattern on axis 1 at –2 SD resembled the normal mean.

The generated mean glaucoma field in cluster 3 had a MD of –8.79 dB (compared to –8.4 average MD for the SITA fields in cluster 3). It also had a superior to inferior a ratio of 1.23. The grayscale of the centroid of cluster 3 looked like an exaggerated version of the cluster 2 centroid. The displays at ±2 SD on the 5 axes were distinctly different from each other and from the patterns in cluster 2 (Figure 3). See Table 2 for the descriptions of the grayscales at the means of clusters 2 and 3 and at ±2 SD on each axis in clusters 2 and 3.

Analysis of SITA Fields Associated With Each Axis

Observation of the fields assigned to an axis revealed a number of generalities. The grayscales of the SITA fields assigned to each axis resembled the generated grayscales at +2 SD and –2 SD on the axis, with the exception of 4 of the 14 patterns on the 7 glaucoma axes

(Table 2). In those 4 patterns, some of the SITA fields resembled the generated fields, and some of the fields had spotty defects that averaged out to give the pattern in the generated field.

The fields assigned to an axis were located in space by their distances in standard deviations in the positive or negative direction from the cluster centroid and by the distance from the axis to which it was assigned, measured by the angle between the axis and the vector from the cluster centroid to the field in question. The fields farther in the positive direction away from the cluster centroid showed increasing depth and enlargement of the pattern associated with the axis (Figure 4). The fields farther in the negative direction had decreasing depth or size of the pattern, as in general they were approaching the location of the normal cluster. The pattern of a field closer to the axis to which it was assigned had a stronger resemblance to the generated axis pattern than the fields located in space farther from the axis.

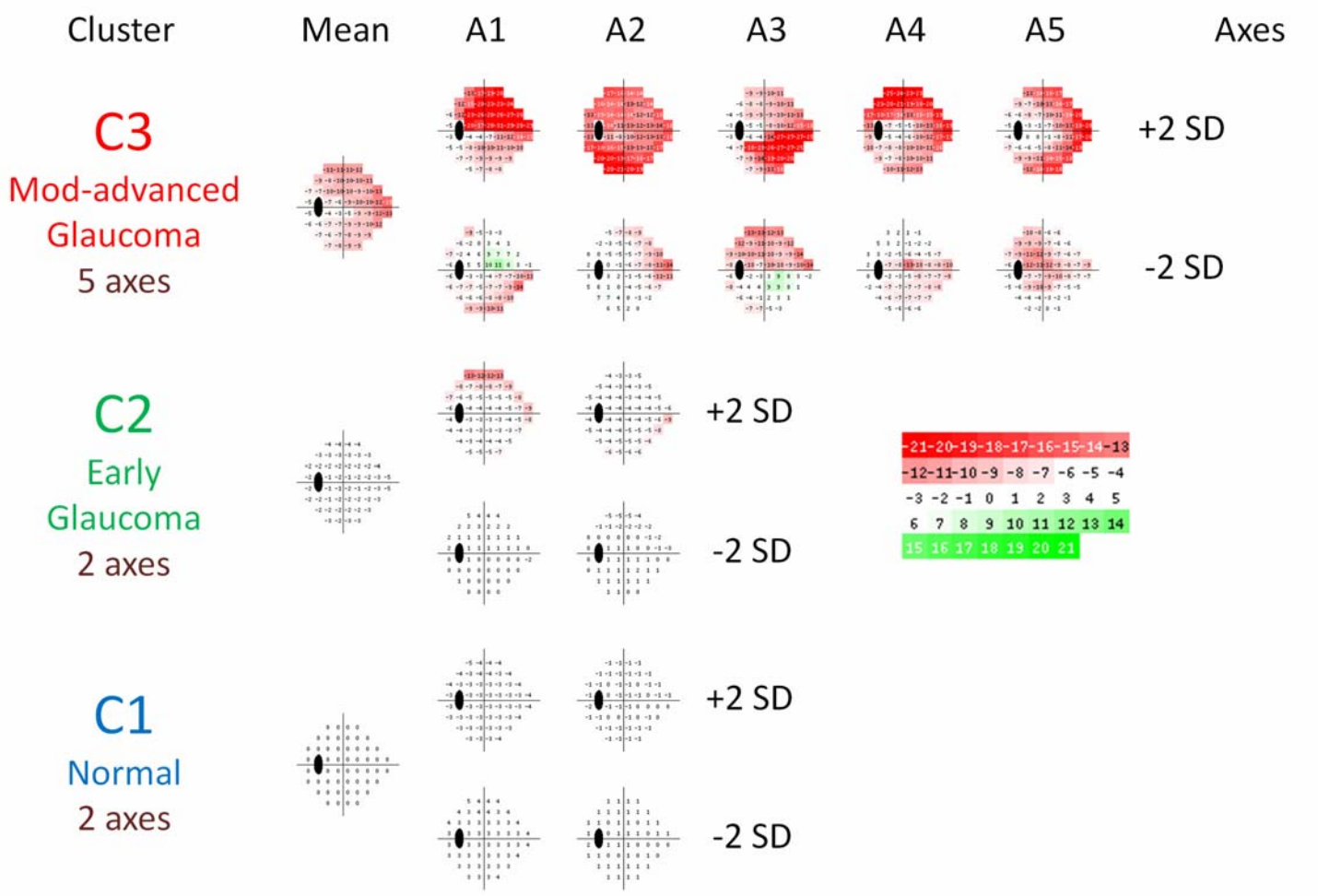

FIGURE 3.

Grayscale displays and plots simulating total deviation plots generated at the mean for each cluster and at –2 and +2 standard deviations (SDs) from the centroid on each axis. The deviation at each visual field location is expressed in decibels. The elevated sensitivity values ≥ (+7) dB are displayed in green, and the depressed sensitivity values ≤ (–7) dB are displayed in red.

TABLE 2. DESCRIPTIONS OF GENERATED PATTERNS ON EACH AXIS AND SITA FIELDS ASSOCIATED WITH EACH AXIS* (SEE FIGURE 3)

	N	GENERATED FIELD ±2 SD PATTERNS	ASSOCIATED SITA FIELDS
Cluster 2 at mean		Mild sup arcuate loss	
Axis 1 at +2 SD	*124*	*Moderate sup peripheral arcuate loss*	*Sup peripheral arcuate*
Axis 1 at -2 SD	161	Sup far peripheral gain	*Scattered locations, 1-3 points
Axis 2 at +2 SD	*148*	*Early inf nasal step loss*	**Nas steps with exceptions*
Axis 2 at -2 SD	136	Early sup far peripheral loss	Sup peripheral mild

TABLE 2 (CONTINUED). DESCRIPTIONS OF GENERATED PATTERNS ON EACH AXIS AND SITA FIELDS ASSOCIATED WITH EACH AXIS* (SEE FIGURE 3)

	N	GENERATED FIELD ±2 SD PATTERNS	ASSOCIATED SITA FIELDS
Cluster 3 at mean		Moderate sup arcuate, milder inf loss	
Axis 1 at +2 SD	*38*	*Deep sup hemifield loss, mild inf loss*	*Many sup hemifield, few inf*
Axis 1 at -2 SD	38	Moderate inf arcuate loss	*Mild arcuates, including temporal
Axis 2 at +2 SD	*25*	*Moderate generalized loss*	*Generalized, 3 or 4 quadrants*
Axis 2 at -2 SD	24	Moderate nas arcuate loss	Nas arcuate
Axis 3 at +2 SD	*34*	*Deep Inf hemifield loss, mild sup loss*	**Many inf defects, few sup*
Axis 3 at -2 SD	22	Moderate sup hemifield loss	Sup arcuate more central
Axis 4 at +2 SD	*36*	*Sup far peripheral arcuate loss*	*Peripheral arcuates, central sparing*
Axis 4 at -2 SD	45	Horizontal midline "arrow shaft" loss	Horizontal midline central
Axis 5 at +2 SD	*35*	*"Arrowhead" loss*	*Nas arrowhead, occasional arcuates*
Axis 5 at -2 SD	26	Sup temporal arcuate loss	Sup temporal arcuates, some other

SITA, Swedish Interactive Thresholding Algorithm.
*****SITA fields associated with an axis closely resembled the generated fields at plus and minus 2 SD except as noted in the boxes with an asterisk.

There were 104 false-negatives out of 1,193 SITA fields in cluster 1. The false-negatives appeared as normal fields to the 2 experts on post hoc review except for 4 fields with a far peripheral superior midline deficit and a few with spotty single-point depressions. There were 56 false-positives out of 569 SITA fields in cluster 2, which contained the mildly abnormal fields. Three false-positives had a single moderate depression in the nasal step region, two had mild temporal wedge depression, and one had a far peripheral superior midline depression. The rest of the fields appeared normal to the experts. The single false-positive in cluster 3 had a single-point moderate depression at the inferior edge of the blind spot.

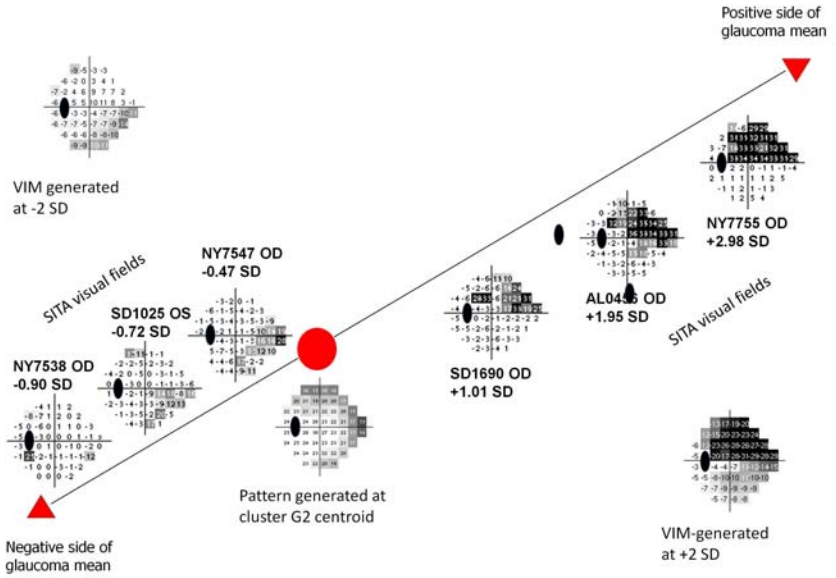

FIGURE 4.

Grayscale display of several eyes assigned to axis 1 in cluster 3 (moderate to advanced glaucoma). The SITA visual fields on each side of the cluster mean resemble each other and also resemble the generated fields on the axis at –2 and +2 SD. As the SITA fields are located more positively, the field defect is more severe. The more severe defects show enlargement and expansion of the same pattern.

DISCUSSION

REPRESENTATION OF DATA STRUCTURE

Without knowing the classification of the fields during the learning process, the various VIM models separated the normal and abnormal fields into 2 or 3 clusters that were validated post hoc to determine if the VIM model gave results consistent with the GHT or PSD criteria for abnormal field. The specificity of 95% and sensitivity of 89% indicated that the chosen model achieved a good match without any knowledge of these criteria. This is a significant improvement in sensitivity over the results with full-threshold testing (specificity 98%, sensitivity 69%).[2] However, the goal of VIM was not accuracy of diagnosis, but rather optimal separation of the data into independent patterns. The expectation was that the best separation of normal and abnormal fields in VIM would create an environment for an optimal set of axes representing the abnormal fields and that these axes would result in a good separation of patterns.

Errors could arise because criteria for determining that an eye had glaucoma were based on the GHT and PSD. Some false-negatives could be explained, for example, by the diminished influence of the superior peripheral locations in triggering an abnormal PSD designation because these areas are influenced by eyelids or refractive lenses, or they could be explained because defects in the temporal area of the field are not included within the GHT analysis. All but one of the false-positives ended up in the cluster of mildly abnormal fields. The single false-positive in the cluster with moderate to severe field abnormalities may have been placed there because of an enlarged blind spot. The majority of the false-positives and -negatives were in a neighborhood of fields that are often difficult to classify. VIM may have placed these fields there because they satisfied some property of the axes more than they satisfied the criteria of GHT or PSD. Since PSD and GHT have their own set of false-negatives and -positives, many of the VIM false-positives and -negatives may actually have been correctly placed. This is something that can be evaluated in a separate study looking at serial visual fields (>2) from the same individual.

Analysis of the axes of the chosen VIM model found that the patterns were distinctly different, that the field defects worsened as the fields were located farther along the positive direction, and that the worsening of a pattern involved deepening and widening of the pattern on an axis (Figure 4). The observed qualitative differences in the grayscale patterns offered visual confirmation of the mathematically derived expression of independence in the data structure. In addition, the patterns were recognizable as typical glaucomatous patterns of field loss, with descriptions such as nasal step, arcuate defect, temporal wedge, altitudinal depression, and central defect. The similarity of the VIM-generated grayscale patterns to those familiar to glaucoma experts and to those found earlier in an independent data set of full-threshold fields[1,2] is promising for the identification of progression[3] and should make the POP approach easier to understand.

The consistency of the observations of VIM applied to 2,085 SITA fields compared to the previous observations of VIM applied to 345 SAP full-threshold fields[1,2] corroborates the robustness of the VIM algorithm applied to different data. The set of normal and glaucomatous fields in this study was 6 times the size of the set in the previous application of VIM. This larger set of normal and glaucomatous fields enabled the formation of axes whose patterns were more distinctly different than those found previously. These findings satisfied the goal of establishing maximally independent yet recognizable glaucomatous field patterns.

A common use of ICA is dimension reduction for the goal of separating true signal from noise. This noise-reducing dimension reduction then becomes a preprocessing step for subsequent processing. The expectation is that the VIM method of dimension reduction will help separate true deterioration of the field from fluctuations not due to progression. We can therefore seek to improve the detection of glaucomatous visual field progression (signal) in measurements that contain fluctuations in the visual fields not caused by progression (noise). We previously used VIM to detect progression of glaucomatous field loss eyes measured by SAP full threshold.[3] In that study, VIM applied to sequential fields of an eye detected progression at least as well as current techniques and possibly with increased sensitivity. As the glaucoma deteriorated in an eye, the fields tended to maintain the same pattern, with deepening and expansion of the pattern.[3]

The SITA fields plus age were reduced by VIM from 53 dimensions to 9 dimensions represented by the 9 resulting axes. The 9 dimensions have the property of being maximally independent. This property and the characteristic of increasing pattern severity along the axes (Figure 4) prepare VIM for the subsequent step of separating true progression of glaucoma from noise in SITA visual fields.

Frequently, statistical analysis of a multifeatured data set relies on multivariate analysis. Multivariate analysis uses linear classification that makes assumptions about the data that may not be true, such as equality of covariance. The reduction of dimensionality from 53 to 9 by VIM is designed to maximize the independence of the synthesized features. This property may permit univariate analysis of the axis showing the most progression.

The progression of SITA visual fields by POP is under analysis. We are currently applying VIM to a large cohort of eyes followed annually by SITA fields in an effort to improve the separation of eyes with progressing glaucoma from eyes with stable glaucoma. The expectation is that a mathematically principled approach will avoid the limitations and bias of a set of rules created by human experts and will find indications of progression not apparent to human experts.

In summary, VIM worked well on SITA fields, separating the SITA fields into distinctly different yet recognizable patterns of glaucomatous field defects. This outcome was instructive, and the outcome properties make VIM a good candidate for detecting change.

ACKNOWLEDGMENTS

Funding/Support: Supported by grants EY08208 (P.A.S.), EY11008 (L.M.Z.), EY13928 (M.H.G.), EY13959 (C.A.G.), and EY14267 (P.A.S.) from the National Institutes of Health; the Eyesight Foundation of Alabama (C.A.G.); the David and Irene Dunn Foundation (M.H.G.); and Alcon Laborataories Inc, Allergan, Pfizer Inc, Merck Inc, and Santen Inc.

Financial Disclosures: None.

Author Contributions: *Design of the study* (M.H.G., P.A.S.); *Conduct of the study* (M.H.G., C.B., L.M.Z., J.L., C.G.); *Management, analysis, and interpretation of the data* (M.H.G., P.A.S., G-J.J., J.H., T-P.J., J.L., C.G.); *Preparation, review, or approval of the manuscript* (M.H.G., P.A.S., R.N.W.)

Conformity With Author Information: The study followed the tenets of the Declaration of Helsinki and was approved by the Institutional Review Boards of the University of California, San Diego, New York Eye and Ear Infirmary, and University of Alabama at Birmingham.

REFERENCES

1. Goldbaum MH. Unsupervised learning with independent component analysis can identify patterns of glaucomatous visual field defects. *Trans Am Ophthalmol Soc* 2005;103:270-280.
2. Goldbaum MH, Sample PA, Zhang Z, et al. Using unsupervised learning with independent component analysis to identify patterns of glaucomatous visual field defects. *Invest Ophthalmol Vis Sci* 2005;46:3676-3683.
3. Sample PA, Boden C, Zhang Z, et al. Unsupervised machine learning with independent component analysis to identify areas of progression in glaucomatous visual fields. *Invest Ophthalmol Vis Sci* 2005;46:3684-3692.
4. Sample PA, Chan K-L, Boden C, et al. Using unsupervised learning with variational Bayesian mixture of factor analysis to identify patterns of glaucomatous visual field defects. *Invest Ophthalmol Vis Sci* 2004;45:2596-2605.
5. Bengtsson B, Olsson J, Heijl A, Rootzen H. A new generation of algorithms for computerized threshold perimetry, SITA. *ACTA Ophthalmol Scand* 1997;75:368-375.
6. Chan K, Lee T-W, Sejnowski TJ. Variational learning of clusters of undercomplete nonsymmetric independent components. *J Machine Learn Res* 2002;3:99-114.
7. Lee T-W, Lewicki MS, Sejnowski TJ. ICA mixture models for unsupervised classification of non-Gaussian sources and automatic context switching in blind signal separation. *IEEE Trans Pattern Anal Mach Intell* 2000;22:1078-1089.
8. Sample PA, Jang G, Jung T-P, et al. Unsupervised machine learning with independent component analysis identifies patterns of glaucomatous visual field loss in SITA fields. *Invest Ophthalmol Vis Sci* 2009;50:E-Abstract 5283.
9. Goldbaum MH, Sample PA, White H, et al. Interpretation of automated perimetry for glaucoma by neural network. *Invest Ophthalmol Vis Sci* 1994;35:3362-3373.
10. Goldbaum MH, Sample PA, Chan K-L, et al. Comparing machine learning classifiers for diagnosing glaucoma from standard automated perimetry. *Invest Ophthalmol Vis Sci* 2002;43:162-169.
11. Sample PA, Goldbaum MH, Chan K-L, et al. Using machine learning classifiers to identify glaucomatous change earlier in standard visual fields. *Invest Ophthalmol Vis Sci* 2002;43:2660-2665.

PEER DISCUSSION

DR. DONALD L. BUDENZ: Dr. Goldbaum and colleagues at UCSD are well known for the application of machine learning classifiers to glaucoma diagnosis. For those not familiar with this methodology, one enters information into a computer which classifies the information based on commonalities and patterns either with or without training (or supervision) on these patterns. The common features create clusters of like patterns, each cluster representing a different pattern. The computer then draws a hyperplane that best separates the clusters so that a new point entered into the classifier has the best chance of ending up in the correct cluster. In a more sophisticated model, the clusters form along vectors, from more normal to more abnormal and the position of individual data points represent how strongly that data point resembles the pattern, or how abnormal it is. Unlike other methods of classifying glaucomatous visual field defects, which are subjective and require human input, machine learning classifiers may be a more objective way to classify complex data such as visual field patterns.

In this particular study by Goldbaum and colleagues, data from 2085 normal and glaucomatous visual fields resulted in 9 different patterns, or vectors, of visual field loss. Although not the specific intent of this study, the vector machine classifier methodology correctly identified 90% of glaucomatous visual fields from known glaucoma subjects and 95% of normal visual fields from normal subjects.

One of the exciting applications of this methodology would be the identification of glaucomatous visual field progression. The idea here is that worsening visual fields would naturally move further down the vector in which the field was placed at diagnosis. This new methodology is called Progression of Patterns (or POP). One of the limitations of visual field testing for progression is long term fluctuation, which is not addressed with vector machine classifier methodology, so one would have to be just as careful in interpreting movement down a vector based on a single or even two fields. Also, it is unclear how intervening abnormalities, like diffuse depression from cataracts, would affect classification or position on the vector.

In summary, the investigators are to be congratulated for applying this novel method for classifying patterns of visual field loss and I look forward to future studies in which one might apply this new method to identifying progression of visual field defects.

ACKNOWLEDGMENTS

Funding/Support: None

Financial Disclosures: Carl Zeiss Meditec

DR. ALLAN J. FLACH: Nothing to disclose. This is really interesting for me because I have never heard this information before. As you were talking, showing the advanced group that was not part of the ellipse and then the different patterns, I was excited about early diagnosis, but I was even more excited about possible insights into pathogenesis of glaucoma. We all assume much of open angle glaucoma is just a chronic disease, but you might have a new and different method of looking to determine if vascular, intraocular pressure, or even systemic factors make the glaucoma different. In other words, your efforts may be trying to teach us all more about pathogenesis or even the etiology, in addition to providing earlier diagnosis.

DR. ROBERT L. STAMPER: Nothing to disclose. I agree with Allan, this is fascinating, and of great interest. We clearly need better ways to distinguish progression from noise. I am a little unclear from what you presented as to the issue of progression. You showed sensitivity and specificity for separating normals from glaucoma and the specificity, if I read it correctly, was about 95% and the sensitivity was about 89%. This suggests that if you have a 5% false positive rate you are going to misclassify more people who are normal than who have glaucoma. If you have a 95% specificity, then that means 5% of your normals will be misclassified as not normal and if the incidence of glaucoma is about 1% or 2% of the population that is twice as many normals will be classified as abnormal than glaucomas who will be so classified. I may be displaying my ignorance here. Could you just quickly explain how this is gonna help us to get the noise out of the repeat visual fields in a way that will allow us to detect progression without repeating the visual fields?

DR. PENNY A. ASBELL: Nothing to disclose. I am also showing a little bit of my ignorance here, so thank you for a very interesting approach of something that might be useful in other disease categories, as well. How do you validate this? I was a little uncertain how you take the information and be sure that you are not sort of giving the answer in terms of distinguishing glaucoma and knowing glaucoma progression. I question whether or not you can take this data and correlate it with other measurements that we typically do in glaucoma, such as intraocular pressure and optic nerve measurements. I was not sure about the correlation and the validation. Thank you.

DR. MICHAEL A. LEMP: I have a conflict of interest. I am a medical officer in a company that is developing a new diagnostic for dry eye. It is of interest to me that we are using the same approach in trying to sort out some of the very difficult questions in diagnosis and assessment of disease severity. I believe this is an outgrowth of what use to be called “Eigen vector analysis”. Evaluating various vectors, finding clusters of clinical data, and looking at these things presents an entirely different way of looking at disease. I believe that is something most of us clinicians have never done before and it has some interesting outcomes. It is just interesting for me to see that another branch of ophthalmology is looking at some of the vexing problems in glaucoma, just like we have in dry eye disease and are using similar types of mathematical analysis. Thank you.

DR. MICHAEL H. GOLDBAUM: Thank you for all of the comments. As far as how to look for progression in so many fields, if you have, let us say over ten years, lots of fields, the eye might be deteriorating at a slow rate and then suddenly drop. Now that sudden increase of deterioration would indicate progression, but if you just look at the slope over the entire time, you might not see it. We would be applying a moving window on our data to look for a sudden increased rate of change.

This approach was not used for diagnosis. The previous work that we have done simplifies learning, and there we were trying to find a diagnosis. We consider that diagnosis is a significant problem, and progression is even more significant, and this approach was set up to look for progression. The way we do that is to concentrate on the axis where there is change. The other axes, where there is not much change, represent noise. By eliminating the other axes, we can reduce the noise and strengthen the signal and thereby improve the signal to noise ratio. That is the purpose of this investigation, and not making a diagnosis.

Now how to determine whether we really have change and compare this to other methods is a difficult problem, because we do not have a gold standard for progression. Perhaps serial stereophotographs will be a good method for determining progression, and that is one of the possibilities that we are considering. Our initial work with this indicates that our method is more sensitive in finding change than the other current methods, but whether this represents real change or not is going to be a difficult problem because of the difficulty in finding a gold standard. As I said, we will probably concentrate on using a change in stereophotographs.

PCA is principal component analysis, which creates orthogonal axes that theoretically are independent, but in fact they are not as independent as you can obtain with independent component analysis, which uses a measurement of independence and then uses that measurement to make sure that the axes are maximally independent. That way, what you have is a series of axes just like you would have with principal component analysis, but because they are maximally independent, you can do a univariant analysis on the one axis which is most involved. That is one of the reasons why this method has been so good at noise reduction in other disciplines.